Research Paper
Computational Methods for Differential Equations
http://cmde.tabrizu.ac.ir
Vol. 12, No. 1, 2024, pp. 149-158
DOI:10.22034/cmde.2023.54929.2283

Numerical simulation of two link robotic manipulator with white and colored noise

Hadiseh Babazadeh[1] **and Parisa Nabati**[2,*]

[1]Faculty of Electrical Engineering, Urmia University of Technology, Urmia, Iran.

[2]Faculty of Science, Urmia University of Technology, Urmia, Iran.

Abstract

The main purpose of this paper is to introduce a new method to analyze the effects of the white and colored noise perturbations on the robotic arms. To show the efficiency of the presented idea the simplest manipulator, two link robotic arm, is considered. Most previous noise analyses of manipulators are done using mechanical or electrical modeling. Applying exact kinematic equations of the robots is the novelty of the proposed research. For this purpose, by adding white and colored noise terms in each angle function of the robotic arm, the end effector linear velocity is studied. Also, mechanical variation's effect on the final velocity in noisy space is considered. The longer the length of the links, the more the noise effect. Analysis of simulation results shows that the root mean square error in 2nd order is more than when angle functions are of the first order. Also, the mean square error is less when colored noise is added in comparison to the white noise. The Matlab programming is used to perform numerical examples to show the efficiency and accuracy of the presented idea.

Keywords. Colored noise, Jacobian, Stochastic differential equation, Two link robot, Velocity kinematics, White noise.

2010 Mathematics Subject Classification. 60H10, 81T80, 68T40.

1. Introduction

Electromechanical devices are used widely in many various fields. An interesting area of these devices is Robotic-arm manipulators. Connecting links with joints and moving them using different kinds of motors makes robotic arms suitable for different applications [12, 20]. The more the number of joints, the more the degrees of freedom (DOF) of the robot, the more flexible arm, and the easier motion in 3D space. Such a manipulator (fig. 1) is a nonlinear system, which is difficult to model and control because of its complex dynamics [19]. So, some assumptions are made to analyze these systems, e.g. the links are regarded to be rigid bodies. To define the end effector situation, a coordinate frame is assigned for each joint, and mathematical relations of rotation or displacement are applied to these frames to construct the position and orientation of the end effector concerning the base (kinematics). As joints move, the end effector changes its position as well as its speed. In fact, the angular/linear speed of the end effector can be defined according to the joint velocities (velocity kinematics) [21]. Many researchers are done studying the kinematics of the different robotic arms, especially famous SCARA or PUMA robots without concern any kind of noise or perturbation [1, 2, 8, 23].

For a manipulator, there are different kinds of noise sources, e.g. motor noise, electrical/controlling circuit noise, environmental noise, and others. So, the arm is performing the defined job in a noisy space. To analyze this case, some studies model the arm mechanically or electrically and try to analyze the model. In [22], the electrical circuit model of the motors is driven, and then the electrical equations are studied considering the noise of model elements. In [10] the movement of the arm (end-effector) in a noisy environment is addressed. Where the environment is modeled and the end effector trajectory is designed or predicted in the presence of noise.

Received: 12 January 2023 ; Accepted: 16 April 2023.
∗ Corresponding author. Email: p.nabati@uut.ac.ir .

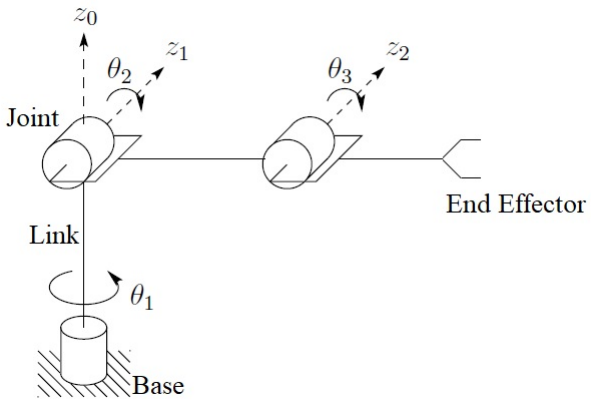

FIGURE 1. Robotic arm manipulator.

In this paper, a try is presented to add a noise source to the real kinematic equations of the robotic arm. It means that the analysis is done on the arm real equations instead of just a mechanical or electrical model. The noise, in general, is added as a random and unpredictable source to the equations. Here the method of noise analysis of robotic arms is of concern. For this reason, just a simple to perform analysis of a simple two-link robot is assumed, and the effect of white/colored noise on the velocity of the end-effector is taken as the final result. Stochastic differential equations (SDEs) were applied to model the systems which can be issued to fluctuations. Diffusion processes were utilized in modeling various phenomena, for instance, filters, noisy electrical circuits, control, and different fields of electrical engineering[9, 11]. Any unwanted disturbance in an electrical signal is called noise. The noise produced by using a digital tool varies significantly as it is generated using numerous distinct outcomes and is unavoidable. So some techniques are wanted to have a look at and examine the noise outcome [17]. The multiplicative noise is used for modeling in wireless communications, signal processing, and radars [3, 18]. Until now, non-white noises are rarely used to model the noise of systems. Because the path of a Wiener process are nowhere differentiable, white noise can not be considered a stochastic process in the usual way however may be approximated via conventional stochastic approaches with extensive spectral bands are generally called colored noise processes. In these conditions, the colored noise was developed for the first time in [24, 25].

Brownian particle velocity stochastic behavior is roughly characterized, and it can be utilized to further identify the precise position of the Brownian particle. The most well-known example of this kind of noise is the Ornstein-Uhlenbeck process. The primary distinction between the Ornstein-Uhlenbeck process and the conventional Wiener process is that the former can explain the position of a particle by accounting for friction; as a result, the mathematical model affected by colored noise is more accurate [26]. References [4, 26] contains extensive information on the Ornstein-Uhlenbeck process and random dynamical systems.

The literature reviews showed that Farnoosh et. al. have described a stochastic perspective of RL electrical circuit using different noise terms [6]. They investigate the parameter estimation for the RL electrical circuit in another paper [7]. Kolarova studies the RLCG cells with colored noise[14]. Nabati and Farnoosh investigated the white and colored noise perturbations on the parameters of the RC and RLC electrical circuits [16]. The organization of this paper is as follows. In section 2, the deterministic model of a two-link robot is presented. The stochastic model with white and colored noise is investigated in section 3. The numerical simulations of the proposed stochastic model are introduced in section 4. Finally, section 5 presents the main conclusions.

2. Problem formulation

Two-link planar arms are the simplest form of a robot. As shown in Figure 2, the arm has two revolute joints and two links plus an end effector. The end effector is considered to be a part of the second link. The forward kinematic model of the arm is established according to Denavit- Hartenberg (DH) parameters. A coordinate frame is assigned

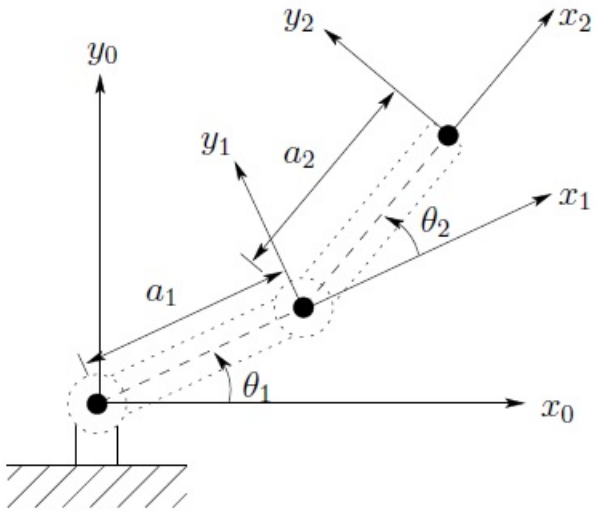

FIGURE 2. Tow link planar robotic arm.

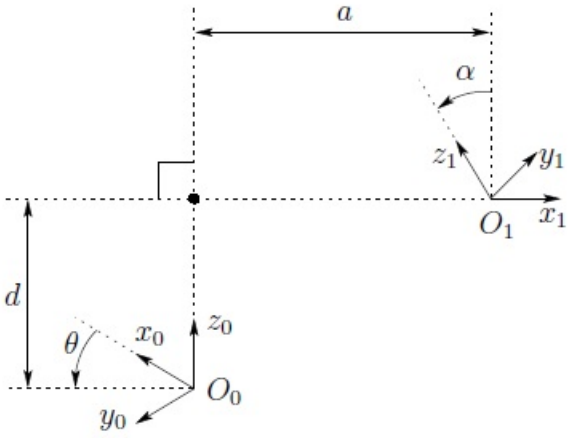

FIGURE 3. Two adjacent coordinates according to DH parameters.

to each robot's joints and the rotation or displacement of each frame is defined according to the base. DH parameters are four parameters defined in the case that the Denavit- Hartenberg convention (below conditions) is met for two adjacent frames of O_0 and O_1 (Figure 3).

DH1: The axis x_1 is perpendicular to the axis z_0.

DH2: The axis x_1 intersects the axis z_0.

DH works with quadruple $\{\alpha_{i-1}, a_{i-1}, d_i, q_i\}$ stand for twist angle, link length, link offset and joint angle respectively. An orthonormal coordinate system has been attached to each link of the manipulator, following DH specifications (Figure 2). The base frame is O_0, and the joint axes z_0 and z_1 are normal to the page. The direction of the x_0 axis is arbitrary. After establishing the base frame, the O_1 frame is set by the DH parameters, where the origin O_1 has been

TABLE 1. DH parameters for the robotic arm.

Link	a_i	α_i	d_i	θ_i
1	a_1	0	0	θ_1^*
2	a_2	0	0	θ_2^*

located at the intersection of z_1 and the page. The final frame O_2 is fixed by choosing the origin O_2 at the end of link 2. Table 1 lists the DH parameters for the robotic arm. According to the table rows, two homogeneous matrices can be formed as follows:

$$A_1 = \begin{bmatrix} \cos\theta_1(t) & -\sin\theta_1(t) & 0 & a_1\cos\theta_1(t) \\ \sin\theta_1(t) & \cos\theta_1(t) & 0 & a_1\sin\theta_1(t) \\ 0 & 0 & 1 & 0 \\ 0 & 0 & 0 & 1 \end{bmatrix},$$

$$A_2 = \begin{bmatrix} \cos\theta_2(t) & -\sin\theta_2(t) & 0 & a_2\cos\theta_2(t) \\ \sin\theta_2(t) & \cos\theta_2(t) & 0 & a_2\sin\theta_2(t) \\ 0 & 0 & 1 & 0 \\ 0 & 0 & 0 & 1 \end{bmatrix}.$$

The T matrices defining coordinates with respect to the origin, are thus given by

$$T_0^1 = A_1,$$

$$T_0^2 = A_1A_2 = \begin{bmatrix} \cos(\theta_1(t)+\theta_2(t)) & -\sin(\theta_1(t)+\theta_2(t)) & 0 & a_1\cos\theta_1(t) + a_2\cos(\theta_1(t)+\theta_2(t)) \\ \sin(\theta_1(t)+\theta_2(t)) & \cos(\theta_1(t)+\theta_2(t)) & 0 & a_1\sin\theta_1(t) + a_2\sin(\theta_1(t)+\theta_2(t)) \\ 0 & 0 & 1 & 0 \\ 0 & 0 & 0 & 1 \end{bmatrix}.$$

Supposing joints are stimulated by a motor and $q(t)$ is the joint variable function (here its angle $\theta(t)$) with respect to time. As the robot moves about, the joint angles and the end effector position and orientation will be functions of time. The linear and angular velocity of the end effector (v_n^0, w_n^0) are related to the vector of joint variables velocity $\dot{q}(t)$.

$$\zeta(t) = J(t)\cdot\dot{q}(t), \tag{2.1}$$

in which $\zeta(t)$ and $J(t)$ are given by:

$$\zeta(t) = \begin{bmatrix} v_n^0 \\ w_n^0 \end{bmatrix} \quad J(t) = \begin{bmatrix} J_v \\ J_w \end{bmatrix}.$$

The relation is shown using the $6n$ Jacobian matrix for an n DOF robot. In the case of two link robotic arm this matrix will be of size 62 and will be written as follows [21]:

$$J(q) = \begin{bmatrix} Z_0\times(O_2-O_0) & Z_1\times(O_2-O_0) \\ Z_0 & Z_1 \end{bmatrix},$$

where the matrix terms are calculated using:

$$O_0 = \begin{bmatrix} 0 \\ 0 \\ 0 \end{bmatrix}, O_1 = \begin{bmatrix} a_1\cos(\theta_1(t)) \\ a_1\sin(\theta_1(t)) \\ 0 \end{bmatrix}, O_2 = \begin{bmatrix} a_1\cos(\theta_1(t)) + a_2\cos(\theta_1(t)+\theta_2(t)) \\ a_1\sin(\theta_1(t)) + a_2\sin(\theta_1(t)+\theta_2(t)) \\ 0 \end{bmatrix},$$

$$Z_0 = Z_1 = \begin{bmatrix} 0 \\ 0 \\ 1 \end{bmatrix}.$$

As a result, the Jacobian matrix will be:

$$J(t) = \begin{bmatrix} -a_1 \sin\theta_1(t) - a_2 \sin(\theta_1(t)+\theta_2(t)) & -a_2 \sin(\theta_1(t)+\theta_2(t)) \\ a_1 \cos\theta_1(t) + a_2 \cos(\theta_1(t)+\theta_2(t)) & a_2 \cos(\theta_1(t)+\theta_2(t)) \\ 0 & 0 \\ 0 & 0 \\ 0 & 0 \\ 1 & 1 \end{bmatrix},$$

where θ_1 and θ_2 show the first and second joints angle function respectively. According to the Jacobian matrix in the two-link robotic arm the end effector linear velocity is in two dimensions and can be obtained as:

$$V^2 = \sqrt{V_x^2 + V_y^2}.$$

Since there is no velocity vector in the z-direction the overall linear velocity will be equal to the vector-sum of velocities on the x and y-direction. The angular velocity is results from the sum of angular velocities of both joints since they have a parallel rotation axis. The main purpose of this research is to analyze the linear velocity of the end effector considering white and colored noise. Also, the relation between the velocity noise and the mechanical length of the robot links is of interest. Hence, mathematical codes according to manipulator kinematics are formed and run to observe these effects.

3. Stochastic model

The end effector linear and angular velocity vectors are related to the derivation of each joint velocity according to the equation (2.1) can be easily stated as the following equation:

$$\begin{bmatrix} V_x(t) \\ V_y(t) \\ V_z(t) \\ W_x(t) \\ W_y(t) \\ W_z(t) \end{bmatrix} = \begin{bmatrix} -a_1 \sin\theta_1(t) - a_2 \sin(\theta_1(t)+\theta_2(t)) & -a_2 \sin(\theta_1(t)+\theta_2(t)) \\ a_1 \cos\theta_1(t) + a_2 \cos(\theta_1(t)+\theta_2(t)) & a_2 \cos(\theta_1(t)+\theta_2(t)) \\ 0 & 0 \\ 0 & 0 \\ 0 & 0 \\ 1 & 1 \end{bmatrix} \begin{bmatrix} \dot{\theta_1}(t) \\ \dot{\theta_2}(t) \end{bmatrix}, \tag{3.1}$$

where a_1, a_2 known as first and second link length respectively. In deterministic models $\theta_i(t)$ for $i = 1, 2$ sometimes are linear functions.

3.1. **The stochastic model with white noise.** Let $(\Omega, \mathcal{F}, \mathbb{P})$ be a fundamental probability space supported by a right continues family of σ-algebras $\{\mathcal{F}_t, t \geq 0\}$. If there may be a few randomness within the each joint variable function, in equation (3.1), then the $\theta_i(t)$ may not be deterministic, however of the form:

$$\theta_i^*(t) = \theta_i(t) + \text{"}white\ noise\text{"} = \theta_i(t) + \sigma_i \omega_i(t), \tag{3.2}$$

in which σ_i is a positive constant known as the noise intensity and $\omega_i(t)$ is an $\mathcal{F}_t$ adapted white noise process. White noise is a type of noise that has a constant power spectral density across all frequencies. It is often referred to as random noise because it has no discernable pattern or structure. It has an alternative distribution of a generalized derivative of a Brownian motion. The process $\omega_i(t)$ is defined formally as $dB_i(t) = \omega_i(t)dt$ and known as a Brownian motion.With substituting equation (3.2) in equation (3.1) we have

$$\begin{bmatrix} V_x(t) \\ V_y(t) \\ V_z(t) \\ W_x(t) \\ W_y(t) \\ W_z(t) \end{bmatrix} = \begin{bmatrix} -a_1 \sin\theta_1^*(t) - a_2 \sin(\theta_1^*(t)+\theta_2^*(t)) & -a_2 \sin(\theta_1^*(t)+\theta_2^*(t)) \\ a_1 \cos\theta_1^*(t) + a_2 \cos(\theta_1^*(t)+\theta_2^*(t)) & a_2 \cos(\theta_1^*(t)+\theta_2^*(t)) \\ 0 & 0 \\ 0 & 0 \\ 0 & 0 \\ 1 & 1 \end{bmatrix} \begin{bmatrix} \dot{\theta_1}(t) + \sigma_1 dB_1(t) \\ \dot{\theta_2}(t) + \sigma_2 dB_2(t) \end{bmatrix}. \tag{3.3}$$

This system of stochastic differential equations has been solved numerically in section 4.

3.2. **The stochastic model with colored noise.** A white noise process cannot be physically realized but can be approximated by conventional stochastic processes with wide spectral bands which are commonly known as colored noise process [15]. Colored noise has a power spectral density that varies with frequency. It is defined as follows:

Definition 3.1. The stochastic process $\xi(t)$ is called colored noise if it is an Orstein-Uhlenbeck process that satisfies the linear additive SDE:

$$\begin{cases} d\xi(t) = -\lambda\xi(t)dt + \sigma dB(t), \\ \xi(0) = \xi_0, \end{cases} \tag{3.4}$$

where λ, σ are positive parameters and ξ_0 is a random variable is independent of a standard Brownian motion.

The equation(3.4) has a unique strong solution

$$\xi(t) = \exp(-\lambda t)\Big(\xi_0 + \sigma \int_0^t \exp(\lambda s)dB(s)\Big). \tag{3.5}$$

The mean, variance and covariance of $\xi(t)$ with some algebraic manipulation can be obtained

$$\begin{aligned} &E(\xi_t) = exp(-\lambda t)E(\xi_0), \\ &var(\xi_t) = \tfrac{\sigma^2}{2\lambda} + (var(\xi_0) - \tfrac{\sigma^2}{2\lambda})exp(-2\lambda t), \\ &cov\big(\xi(s), \xi(t+s)\big) = \Big(var(\xi_0) + \tfrac{\sigma^2}{2\lambda}(exp(2\lambda s) - 1)\Big)exp(-\lambda(2s+t)), \end{aligned} \tag{3.6}$$

respectively [5]. Now, the noise term in equation (3.2) is considered as a colored noise process. Therefore we have,

$$\theta_i^*(t) = \theta_i(t) + \text{"}colored\ noise\text{"} = \theta_i(t) + \sigma_i\xi_i(t), \tag{3.7}$$

With substituting this in equation (3.1) we have

$$\begin{bmatrix} V_x(t) \\ V_y(t) \\ V_z(t) \\ W_x(t) \\ W_y(t) \\ W_z(t) \end{bmatrix} = \begin{bmatrix} -a_1\sin\theta_1^*(t) - a_2\sin(\theta_1^*(t) + \theta_2^*(t)) & -a_2\sin(\theta_1^*(t) + \theta_2^*(t)) \\ a_1\cos\theta_1^*(t) + a_2\cos(\theta_1^*(t) + \theta_2^*(t)) & a_2\cos(\theta_1^*(t) + \theta_2^*(t)) \\ 0 & 0 \\ 0 & 0 \\ 0 & 0 \\ 1 & 1 \end{bmatrix} \begin{bmatrix} \dot{\theta_1}(t) + \sigma_1 d\xi_1(t) \\ \dot{\theta_2}(t) + \sigma_2 d\xi_2(t) \end{bmatrix}. \tag{3.8}$$

The numerical simulation of this system has been done in the next section.

4. Numerical simulation

Since some of the SDEs can not be solved analytically, hence researchers have searched numerical solutions for simulated them [16]. Now the stochastic Euler scheme is used based on the numerical strategies for ODEs. For a given positive integer n, allow $\Delta t = \frac{T}{n}$ and consider the partitions $\Pi_n = \{0, t_1, t_2, ..., t_n = T\}$ of the interval $[0, T]$. At first we simulated the colored noise process using the Euler scheme for equation (3.4):

$$\xi(t_{i+1}) = \xi(t_i) - \lambda\xi(t_i)\Delta t + \sigma\Delta B(t_i), \tag{4.1}$$

where $\Delta B(t_i) = B(t_{i+1}) - B(t_i) \sim N(0, \Delta t)$. Through generating the mean of a thousand sample path of a normal distribution in Matlab, the simulated $\xi(t_i)$ can be resulted. Then the discrete Euler method is used for simulating the equations (3.3) and (3.8).

According to the defined constraints on the initial and final velocities, or acceleration, different functions can be used for $\theta_1(t)$ and $\theta_2(t)$. In this research two different conditions are regarded, a first order function, and a second order one. In both cases the two functions are supposed to be the same to avoid more complexity.

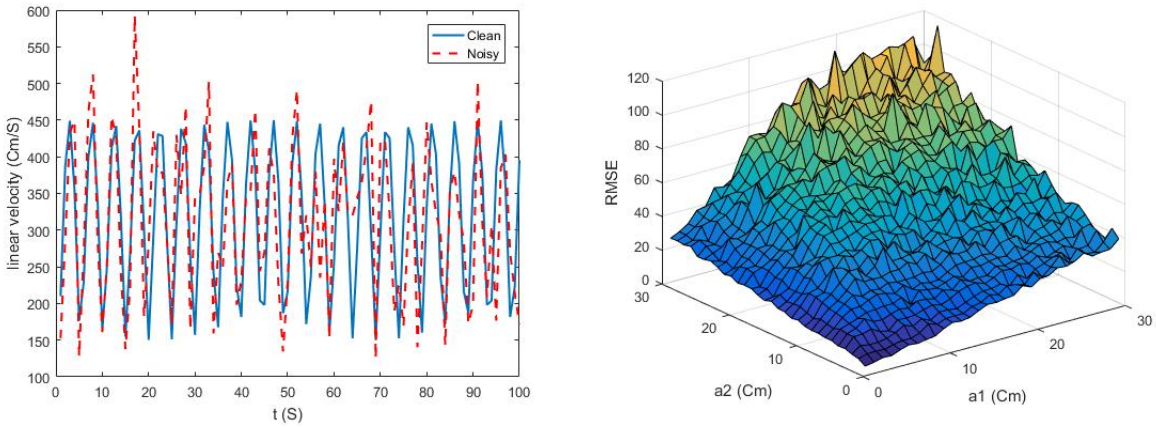

FIGURE 4. left(a): Comparison the final velocity with white noise and without noise, right(b): The RMSE of the clear and noisy end effector velocity.

TABLE 2. MSE for different noise term intensity with white and colored noise.

Simulations	σ	MSE (white noise)	MSE (Colored noise)
Simulation study 1	0.1	57.76	3.71
	0.5	1.34e+3	1.02e+3
	1	4.63e+3	3.41e+3
Simulation study 2	0.1	298.21	11.06
	0.5	7.04e+03	4.45e+03
	1	2.38e+04	4.69e+04

4.1. **Simulation study 1.** In the first case the initial angle is set to be 10 degrees, with 5 degrees increment at each second. The $\theta_1(t)$ and $\theta_2(t)$ will be as:

$$\theta_1(t) = \theta_2(t) = 5t + 10. \tag{4.2}$$

With two different white and colored noise terms respectively. In all simulations the physical size of the links is in Centimeter, so the final velocity will be in Cm/S. Figure (4) shows the simulation results, when $\theta_1(t)$ and $\theta_2(t)$, are first-order and the White noise is added to the equations. In Figure (4-a) the final velocity with and without noise are brought and their difference is shown. As a factor to show the difference of these two plots, their MSE is calculated for different noise intensities (Table 2) and for a typical length of 20 Cm for each link.
Another simulation is run where the link lengths are swept from 1 to 30 Cms. The RMSE of the clear and noisy end effector velocity is calculated and brought in the Figure (4-b) as a surface. As is shown, the RMSE increases, increasing link length. So, maximum tolerable RMSE can be another factor to set the mechanical dimensions, in addition to other parameters.
The same set of simulations is done when the added noise is a colored one. The result of the linear velocity with and without noise is shown in Figure (5-a). Also, the RMSE of the final velocity when the lengths are swept is shown in the Figure (5-b).

Simulation study 2. In the next case, again the initial angle is set to be 10 degrees and $\theta_1(t)$ and $\theta_2(t)$ are considered to be:

$$\theta_1(t) = \theta_2(t) = 0.1t^2 + t + 10, \tag{4.3}$$

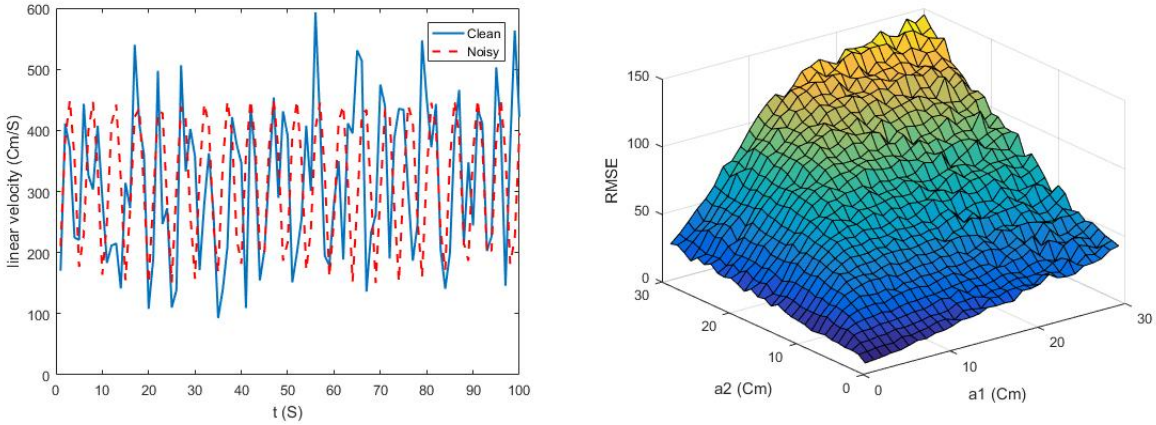

FIGURE 5. left(a): Comparison the final velocity with colored noise and without noise, right(b): The RMSE of the clear and noisy end effector velocity.

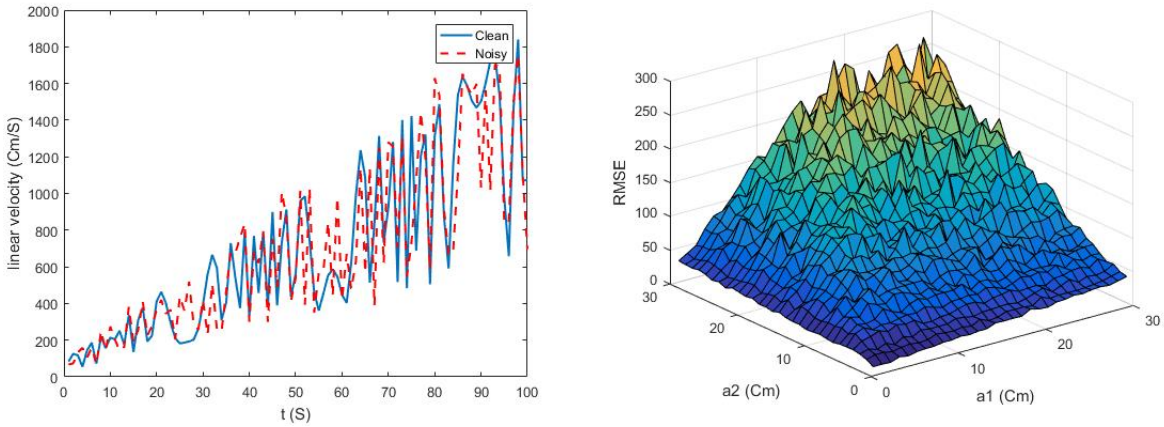

FIGURE 6. left(a): Comparison the final velocity with white noise and without noise, right(b): The RMSE of the clear and noisy end effector velocity.

Here the average velocity will increase with time. In figures (6) and (7) simulation results are done for both white and colored noise respectively. In these figures velocity of the end, the effector is plotted in two cases of noisy and clean conditions, then the RMSE of these two are plotted in a surface, while the physical length of links is swept.

5. CONCLUSION

Here, a method is presented to analyze the robotic arm in the presence of noise. Since the emphasis is on the method rather than the case, the simplest form of the robotic arm, two-link manipulator, is considered. To perform the analysis both white and colored noise are added to the kinematic equations of the arm and the end effector linear velocity is compared in these cases. Also, the RMSE of end effector velocity with and without noise is analyzed, where the physical length of the links is swept. It is found that in the practical implementation of this robot, the link length should be kept as minimum as possible to have fewer noise effects. According to simulations, the colored noise effect is more severe than the white noise. This effect is also bolder when the angle function order increases. Analysis of simulation results shows that the RMSE in 2nd order equations is more than when angle functions are of the first

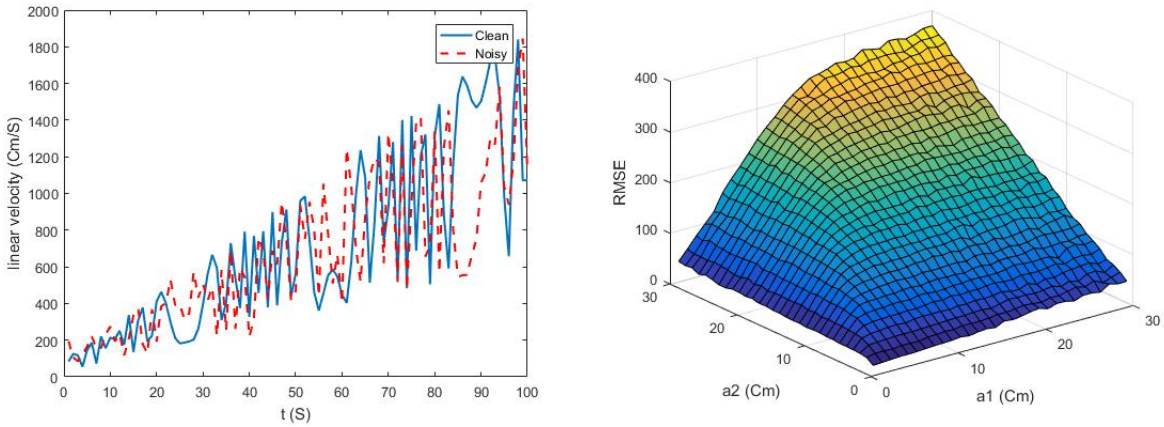

FIGURE 7. left(a): Comparison the final velocity with colored noise and without noise, right(b): The RMSE of the clear and noisy end effector velocity.

order. To extend this study, the proposed analysis can be applied to other robotic structures and different kinematic chains.

REFERENCES

[1] A. Aleksandr and K. Sutyrkina, *On the Position and Stationary Motion Stabilization Problems of a Two-Link Robot Manipulator*, 1st International Conference on Control Systems, Mathematical Modelling, Automation and Energy Efficiency (SUMMA) IEEE, (2019).

[2] Ch. K. Alexander and M. N. D. Sadiku, *Vibration and Kinematic Analysis of Scara Robot Structure*, Diyala Journal of Engineering Sciences, *6* (2013), 127–143.

[3] R. Ashkiani, A. Mahmoudi, M. Karimi, and K. Ansari-Asl, *Closed-Form Estimator for Frequency Estimation of Complex Sinusoidal Signals in Multiplicative and Additive Noise*, Circuits, Systems, and Signal Processing, (2020).

[4] T. Caraballo and X. Han, *Applied Nonautonomous and Random Dynamical Systems, Applied Dynamical Systems*, Springer International Publishing, (2016).

[5] L.C. Evans, *An Introduction to Stochastic Differential Equations*, AMS, (2013).

[6] R. Farnoosh, P. Nabati, R. Rezaeyan, and M. Ebrahimi, *A stochastic perspective of RL electrical circuit using different noise terms*, The International Journal for Computation and Mathematics in Electrical and Electronic Engineering, *30* (2011), 812–822.

[7] R. Farnoosh, P. Nabati, and A. Hajrajabi, *Parameter estimation for RL electrical circuits based on least square and Bayesian approach*, The International Journal for Computation and Mathematics in Electrical and Electronic Engineering, *31* (2012), 1711–1725.

[8] A. Fazli and M. H. Kazemi, *Manipulator Dynamic Nonlinearity Approximation Based on Polytopic LPV Modeling for Robot Tracking Control Problem*, Iranian Journal of Science and Technology, Transactions of Electrical Engineering, *46* (2022), 537–547.

[9] T. R. Field and R. J. A. Tough, *Stochastic dynamics of the scattering amplitude generating K-distributed noise*, J. Math. Phy., *44* (2000), 5212–5223.

[10] D. Guo, F. Xu, L. Yan, Z. Nie, and H. Shao, *A New Noise-Tolerant Obstacle Avoidance Scheme for Motion Planning of Redundant Robot Manipulators*, Front. Neurorobot, (2018).

[11] D. Ham and A. Hajimiri, *Complete noise analysis for CMOS switching mixtures via SDEs*, IEEE Custom Integrated circuits conference, (2000), 439–442.

[12] K. Jahnavi and P. Sivraj, *Teaching and learning robotic arm model, International Conference on Intelligent Computing*, Instrumentation and Control Technologies, IEEE, (2017), 1570–1575.
[13] M. Kaur, S. Sondhi, and V. K. Yanumula, *Kinematics Analysis and Jacobian calculation for six Degrees of Freedom Robotic Arm*, IEEE 17th India Council International Conference (INDICON), (2020).
[14] E. Kolarova and L. Brancik, *Confidence intervals for RLCG cell influenced by coloured noise*, The International Journal for Computation and Mathematics in Electrical and Electronic Engineering, *36* (2017), 838–849.
[15] P. Nabati, *A simulation study of the COVID-19 pandemic based on the Ornstein-Uhlenbeck processes*, Computational Methods for Differential Equations, *10* (2022), 738–745.
[16] P. Nabati, and R. Farnoosh, *Stochastic approach for noise analysis and parameter estimation for RC and RLC electrical circuits*, Int. J. Nonlinear Anal. Appl, *12* (2018), 433–444.
[17] P. Nabati, H. Babazadeh, and H. Azadfar, *Noise analysis of Band Pass Filters using stochastic differential equations* , The International Journal for Computation and Mathematics in Electrical and Electronic Engineering, *38* (2019), 693–702.
[18] C. Shi, F. Wang, M. Sellathurai, and J. Zhou, *Low probability of intercept-based distributed MIMO radar waveform design against barrage jamming in signal-dependent clutter and coloured noise*, IET Signal Proc., *13* (2019), 415–423.
[19] B. Siciliano and O. Khatib, *Springer Handbook of Robotics*, Springer, (2008).
[20] B. Siciliano, L. Sciavicco, L. Villani, and G. Oriolo, *Robotics: modelling, planning and control, Springer Science and Business Media*, (2010).
[21] M. W. Spong, S. Hutchinson, and M. Vidyasagar, *Robot Modeling and Control*, Wiley, (2005).
[22] M. Sung Ahn, H. Chae, D. Noh, H. Nam, and D. Hong, *Analysis and Noise Modeling of the Intel RealSense D435 for Mobile Robots*, 16th International Conference on Ubiquitous Robots (UR), (2019).
[23] M. E. Uk, F. B. Sajjad Ali Shah, M. Soyaslan, and O. Eldogan, *Modeling, control, and simulation of a SCARA PRR-type robot manipulator*, Scientia Iranica B, *27* (2020), 330–340.
[24] G. Uhlenbeck and L. Ornstein, *On the theory of Brownian motion*, Physics Review, *36* (1930), 823-841.
[25] M. Wang and G. Uhlenbeck, *On the theory of Brownian motion. II*, Reviews of Modern Physics,*17* (1945), 323–342.
[26] X. Zhang and R. Yuan, *Pullback attractor for random chemostat model driven by colored noise*, Applied Mathematics Letters, (2020).